Journal of Computational Biology and Bioinformatics Research Vol. 1(1) pp. 001-010, November, 2009
Available online http://www.academicjournals.org/JCBBR

Full Length Research Paper

Chloride anation reaction of aqua (diethylenetriamine) platinum (II): Density functional studies "Dedicated to Prof. H. B. Gray"

Partha Sarathi Sengupta[1*], Snehasis Banerjee[2] and Ashish Kumar Ghosh[3]

[1]Chemistry department, Vivekananda Mahavidyalaya, Burdwan, India, 713103.
[2]Darjeeling Government College India, Darjeeling, 734101, India.
[3]Central Institute of Mining and Fuel Research Institute, Dhanbad, India 828108.

Accepted 2 October, 2009

The nucleophilic and solvolytic path for the chloride anation reaction of aqua(diethylenetriamine)platinum (II) is computationally investigated at the Hartee-Fock (HF) and Density functional theory (B3LYP and mPW1PW91) of levels of calculation in gas phase and on the self- consistent reaction field (SCRF) model. All the stationary points are fully optimized and characterized. The kinetic and thermodynamic properties of all the species involved are investigated and compared with the available experimental data. The transition state is described by local reactivity descriptors. A point of inflection of Fukui function and local softness of the incoming nucleophile for both the solvolytic and nucleophilic path at the transition state (Saddle point), corresponds to both bond breaking and bond making processes. The existence of the solvolytic path (k_1) along with nucleophilic path (k_2) has been supported by DFT studies. From the enthalpy of activation ($\Delta H^{\neq}$), entropy of activation ($\Delta S^{\neq}$) and the structures of the transition states, an inter change associative mechanism (I_a) is established for both nucleophilic and solvolytic path for the chloride anation reaction

Key words: Anation reactions, aqua (diethylenetriamine) platinum (II), DFT, self consistent reaction field, Fukui function.

INTRODUCTION

Theoretical and computational studies of transition metal complexes in solution are of great importance due to their applications in drug design, organometallic energetics, kinetics and in industrial processes (Carloni et al., 2000; Wong et al., 1999; Zeigler, 1995; Michelle et al., 2000). The kinetics of ligand substitution reaction of platinum (II) has shown to follow a two term rate law.

$PtX_3L + Y \longrightarrow PtYX_3 + X$
$Rate = (k_1 + k_2[Y])[PtX_3L]$

The k_2 term relates the associative bimolecular attack of the nucleophile Y on the substrate, the first order rate constant is known to involve the associative solvolysis, followed by rapid anation. Grey et al. (1962) have shown that for the complex $[Pt(dien)Cl]^+$ in aqueous solution proceed through the solvolytic path and $[Pt(dien)(H_2O)]^+$ is the active intermediate of the reaction. The kinetics of the same reaction was revisited by Kotowski et al. (1980)and they demonstrate that $k_{2(obs)}$ is adequately represented by $k_2[Y]$ and appearance of k_1 is within the experimental error limit.

In the present work, the author attempts to analyze the chloride anation reaction via nucleophilic path (1) along with the solvolytic path (2), by *ab-initio* and Density Functional theory

$$[Pt(dien)(H_2O)]^{2+} + Cl^- \xrightarrow{k_2} [Pt(dien)(Cl)]^+ + H_2O \quad (1)$$

$$[Pt(dien)(H_2O)]^{2+} + H_2O \xrightarrow{k_1} [Pt(dien)(H_2O)]^{2+} + H_2O \quad (2)$$

The structures, thermodynamic properties and rate constants were calculated as a function of different level of theory and compared with the experimental data. The solvent effect on thermodynamic and kinetic parameters for this reaction was analyzed in Onsager SCRF model. Finally, the nature of the transition state was described by local reactivity descriptor.

*Corresponding author. E-mail: anapspsmo@yahoo.co.in.

METHODOLOGY

Full unconstrained geometry optimization and frequency calculation for all the distinct species involve in the chloride anation reaction of aqua(diethylenetriamine)platinum(II) have been carried out at the Hartee-Fock (HF) and two Density Functional methods. These are three parameter fit non-local correlation provided by LYP expression and VWN functional III for local correction and exchange functional suggested by Becke (1988,1993,1996), Perdew et al. (1992, 1994), Vosko et al. (1980)] [B3LYP] b) modified Perdew-Wang exchange and Perdew-Wang 91 correlation (MPW1PW91) Adamo et al. (1998). The standard split valence basis set 6-31G (d) (Dtchfield et al., 1971; Hehre et al., 1972) was applied for O and H, N, C and Cl atoms. The relativistic effective core potential (ECP) and associated valence double ξ basis set of Hay and Wadt (Hay et al., 1985), Wadt et al. (1985) (LANL2DZ) was employed for Pt. This includes electrons in the 6s, 6p, and 5d orbitals. All stationary points located on the potential energy surface were characterized as minima (no imaginary frequencies) or first order transition state (characterized by having one imaginary frequency) through harmonic frequency calculations. To gain deeper insight into the reaction pathway, the intrinsic reaction coordinate (IRC) was calculated using Gonzalez–Schlegel second order path following algorithm (Gonzalez et al., 1989, 1990) starting from the optimized transition state structure with a step size 0.100 (a. m. u.)$^{1/2}$ bohr. The minimum energy path used in IRC is defined as the path that would be taken by a classical particle sliding downhill with infinitesimal velocity from the transition state to each minima. Thermal contributions to the energetic properties were also calculated at 298.15 K and 1 atm.

To incorporate the solvent effects in this reaction, self-consistent reaction field model of Onsager (1936), Wong et al. (1991, 1992) has been utilized. In Onsager reaction field model, the solvent is considered as a continuous unstructured dielectric with a given dielectric constant surrounding a solute embedded in a spherical cavity. The rate constant (*k*) have been evaluated according to Eyring's transition state theory,

$$k(T) = (k_B T)/h \exp(-\Delta G^{\ddagger}/RT)$$

where k_B is the Boltzmann constant, T the absolute temperature and h the Planck constant. $\Delta G^{\ddagger}$ is the free energy of activation for each step.

The density–functional theory (Parr et al., 1989; Lewars, 2003) is highly pertinent for chemical concepts. The electronic chemical potential was defined as $\mu = (\partial E/\partial N)_V$, where E and V are the energy of the system and external potential due to the nuclei respectively with N number of electrons. The negative of the electronic chemical potential, μ, that is $-\mu$ is the electronegativity of the species. The hardness of the system has been defined as $2\eta = (\partial\mu/\partial N)_V$. These are the global properties. In order to understand the reaction mechanism, local parameters are very important which varies from point to point and be a measure of reactivity of the different sites in a supermolecule. Parr and Yang (1989) introduced frontier electron density, $\rho(r)$ of the frontier orbital concept of Fukui into the DFT theory (Parr et al., 1989). They defined Fukui function, the space dependent local function, as $f(r) = [\partial\rho(r)/\partial N]_v = [\delta\mu/\delta v(r)]_N$. This measures the sensitivity of the system's chemical potential to an external perturbation at a particular point in a molecular species, with the change of number of electrons.

In chemical reaction, change of electron density changes from one species to another occurs at the transition state. The addition or removal of electron to LUMO or HOMO of the species respectively, the Fukui Function is therefore related to the properties of Frontier orbital (HOMO and LUMO).

The approximate definition of chemical potential μ and chemical hardness η of the system can be obtained by the method of finite difference. These are- $\mu = \chi = (I.E. + E.A.)/2$. $\eta = (I.E. - E.A)/2$, where χ, I. E. and E. A. are the electronegativity, vertical ionization potential and electron affinity of the system.

Within the validity of Koopman's theorem (Szabo et al., 1996) for closed shell electronic systems, the frontier orbital energies is expressed as

$-\varepsilon_{HOMO}$=I. E. and $-\varepsilon_{LUMO}$=E. A.

Due to the discontinuity of electron density $\rho(r)$ with respect to the number of electrons, N, the finite difference method leads three different type of Fukui Function for a system, these are; $f^{-}(r) = \rho_N(r) - \rho_{N-1}(r)$ for electrophilic attack, $f^{+} = \rho_{N+1}(r) - \rho_N(r)$ for nucleophilic attack and $f^{0} = ½[\rho_{N+1}(r) - \rho(r)]$ for radical attack. In practice, the condensed Fukui function (Geerlings et al., 2003; Chattaraj et al., 2005) for an atom k in the molecule was determined. The Fukui Function has therefore used to predict and rationalize the variation of reactivates in different sites of the molecule concerned. The condensed Fukui Function measures the sensitivity of small changes in the number of electrons at atom k in HOMO and LUMO.

They are expressed as $f_k^{+} = [q_k(N+1) - q_k(n)]$, $f_k^{-} = [q_k(N) - q_k(N-1)]$ and

$f_k^{0} = 1/2[q_k(N+1) q_k - (N-1)]$

The Fukui function and local softness are related as $s(r) = f(r).\mathbf{S}$

where **S** is the global softness and is the inverse of global hardness, $\mathbf{S} = 1/2\eta = 1/2(\partial N/\partial\mu)_V$.

The philicity parameter is also another local parameter and has been defined as

$\omega = \mathbf{W}. f(r)$ where W is the global philicity**.**

To determine the Fukui function and local softness, separate calculations were done for N, (N+1) and (N-1) electron system with the same geometry along the IRC path. The Mulliken population analysis scheme was used for the necessary charges. The B3LYP protocol and 6-31(G) basis set have been used for these calculations. All the quantum mechanical calculations have been carried out with the GAUSSIAN 03(RevisionC.02), program (Frisch et al., 2004, GAUSSIAN 03)

RESULTS AND DISSCUSSION

Structural analysis

Figure 1 shows all optimized structures found on the potential energy surface for the species involved in the chloride anation reaction of aqua(diethylenetriamine)-platinum(II). To save the space, only the B3LYP structures are shown. A systematic search for the intermediate structures was done and five stationary points along the reaction pathway were found as can be seen in Figure 1. The reactant molecule shows quasi square planar geometry around the central Pt atom. The three Pt -N bond lengths are 2.031, 2.098 and 2.099 Å and Pt -O bond

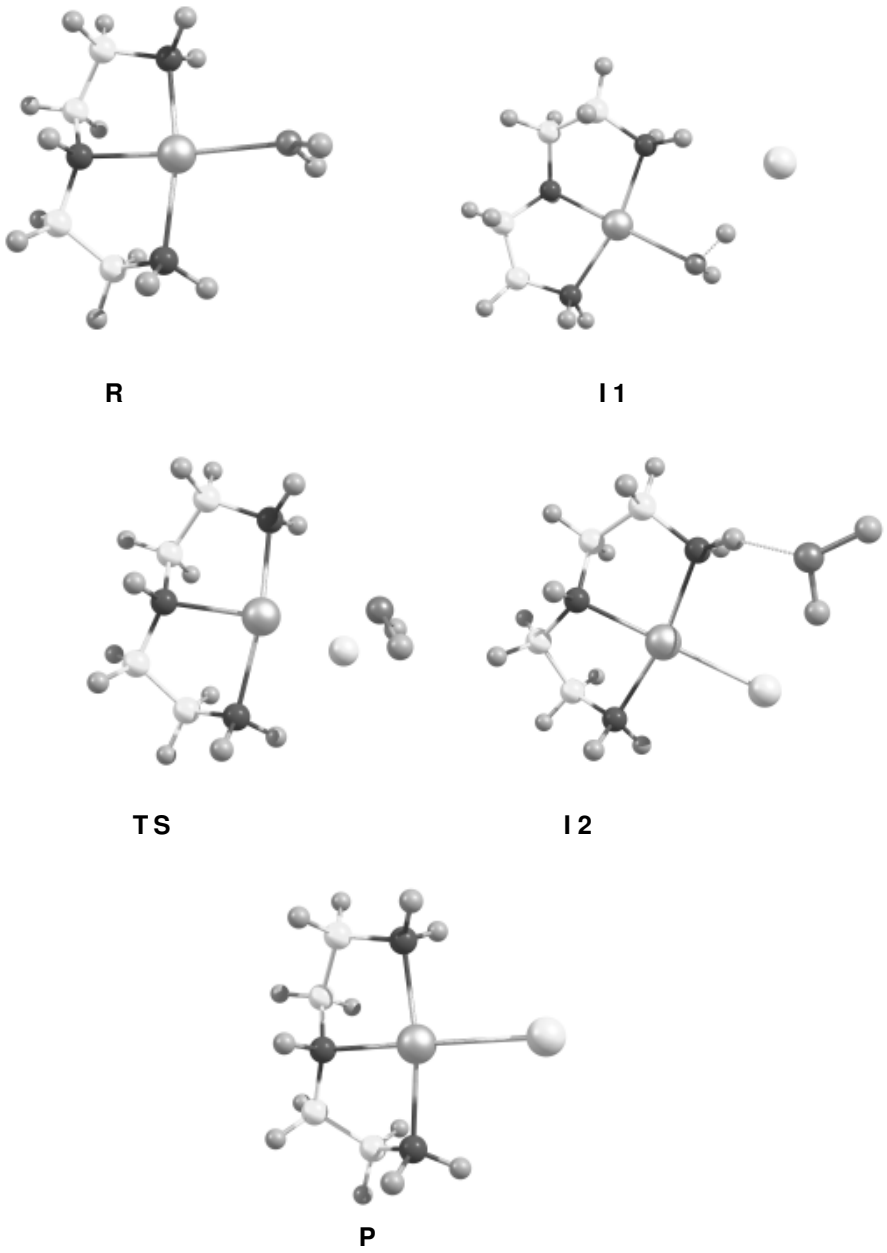

Figure 1. B3LYP optimized structures for species involved in the nucleophilic path for the chloride anation reaction of $[Pt(dien)(H_2O)]^{2+}$

length is 2.14 Å. O-H bond lengths are 0.976 and 0.977 Å at B3LYP level of theory. The bond angles ∠N(T)- Pt –N_2, ∠N(T)- Pt –N_3 and ∠N_2- Pt –N_3, are 83.21°, 84.26° and 165.68° respectively. The ∠O-Pt-N_2 and ∠O-Pt-N_3 bond angles are 101.01° and 91.5° respectively. Both the five member rings of diethylenetriamine (dien) bound with platinum are out of plane with N-C-C-N dihedral angles 39.15° and 51.05° degrees respectively. The structural parameter of the aqua ion $[Pt(dien)(H_2O)]^{2+}$ are unique (Briton et al., 1982) (Table 1) as X ray crystallographic data of this ion was unavailable due to the synthetic problem.

In the intermediate **I1**, $[Pt(dien)(H_2O)]^{2+}$…Cl, the incoming chloride ion is weakly hydrogen bonded with the hydrogen of the aqua ligands at a intermolecular distance of 1.907 Å . The O-H bond distance changes from 0.975 to 1.038 Å. The angle ∠O-H-Cl is 171.2° degrees. The existence of hydrogen bond was supported by the depression of stretching frequencies by 510 cm^{-1} (Cotton et al., 1999).

In this substitution reaction, a five-coordinated trigonal-bi-pyramid like transition state with a small angle (∠ leav-

Table 1. Structural data for optimized aqua ion, $[Pt(dien)(H_2O)]^{2+}$ in different protocol in gas phase. In parentheses are the respective values in Onsager reaction field model.

Bond lengths (Å)	HF	B3LYP	mPW1PW91
Pt-N(T)[a]	2.031(2.032)	2.029(2.031)	2.012(2.009)
Pt-N_2	2.101(2.094)	2.105(2.098)	2.075(2.0746)
Pt-N_3	2.098 (2.108)	2.098(2.099)	2.075(2.0753)
Pt-O	2.148 (2.143)	2.148(2.141)	2.123(2.119)
N(T)-C_3	1.524 (1.505)	1.512(1.511)	1.522(1.5107)
C_3-C_4	1.531 (1.529)	1.53(1.531)	1.522(1.523)
N(T)-C_5	1.512(1.493)	1.512(1.511)	1.519(1.511)
N(T)-H	1.020(1.018)	1.025(1.025)	1.024(1.0235)
C_5-C_6	1.529(1.526)	1.530(1.531)	1.522(1.5229)
N-H	1.021(1.009)	1.024(1.025)	1.021(1.022)
O-H	0.975(0.956)	0.975(0.975)	0.972(0.9723)
C-H	1.095(1.094)	1.092(1.092)	1.092(1.092)
Bond angles(in degrees)			
N(T)-Pt-N_2	83.09 (83.21)	83.09(83.21)	83.32(83.36)
N_2-Pt-N_3	84.25(83.66)	84.24(84.26)	84.46(84.48)
N_2-Pt-O	91.54(91.01)	91.54(91.57)	91.50(91.46)
N_3-Pt-N_2	165.6 (164.89)	165.60(165.68)	165.99(166.06)
N(T)-Pt-O	179.8(179.9)	179.9(179.93)	179.97(180.01)
Dihedral angle			
N(T)-C_3-C_4-N_2	39.28 (39.68)	39.28(39.15)	39.82(39.66)
N(T)-C_5-C_6-N_3	51.22(51.52)	51.22(51.05)	51.53(51.44)

a N(T) is the trans nitrogen with respect to the H_2O.

ing H_2O- Pt - entering Cl that is, 70.14° was found. The TS structure has an imaginary frequency of -129.1 cm^{-1} computed at B3LYP level of theory (Foresman et al., 1996) in which Pt - O (2.341 Å) bond is breaking and Pt - Cl (2.728 Å) bond is forming, the Pt - N(T) bond length in the equatorial plane has larger value than the two axial Pt - N bond length (Figure 2(a) of supporting information). The imaginary frequency at mPW1PW91 level is -130.8 cm^{-1}.

In the intermediate structure **I2**, the leaving aqua ligand, H_2O is hydrogen bonded with intermolecular distance of 1.759 Å, the O atom of H_2O and one of the amine hydrogen of dien are involved in hydrogen bonding. The leaving H_2O is above the quasi-square plane of the complex with N-H…O bond angle 157.6° and the two five membered (Pt-N-C-C-N) ring of the diethylenetriamine ligand are on the opposite side of the leaving H_2O.

This anation reaction was characterized by replacement of H_2O by chloride ion (Cl^-) and proceed via a collision between the reactant $[Pt(dien)(H_2O)]^{2+}$ with the nucleophilc species Cl^- . In such substitution process, a five coordinated distorted trigonal bi-pyramid like transition structure, with entering ligand, leaving ligand and the metal complex being weakly bound was found. This was found to be true from the structural analysis (Table 1). The small angle between entering H_2O and leaving Cl^- minimizes the repulsion between the d orbital electrons of Pt and the electron pairs of entering and leaving group.

From structural analysis for the transition state (Table 1 of supporting information), it was concluded that the main geometric change took place in the equatorial plane of the transition structure (in both gas and SCRF model). In the d^8 trigonal-bi-pyramid transition state, there occurs greater interaction among the filled dπ orbital electrons with the equatorial ligands compared to the axial ligand. Henceforth dπ -pπ* back bonding and dπ -pπ nonbonding repulsion affect the trigonal plane mainly (Atwood, (1997).

In the product $[Pt(dien)Cl]^{+1}$, Pt atom is tetra-coordinated, the angles around the central Pt atom are deviated from their optimal values. The optimized parameters for the product are compared with X-ray crystallographic data (Briton et al., 1982) (Table 2).

The geometries I and II [Figure 3(a), curve E) in intrinsic reaction coordinate were fully optimized at B3LYP level of theory and were found to be the correct intermediate structures (**I 1** and **I 2**).

Population analysis of the transition state from the optimized structure in B3LYP levels of theory reveals that main contribution of HOMO and LUMO comes from d atomic orbital of Pt atom (Figure 2a). It was also observed that through out the reaction path, the energy of HOMO remain constant but the energy of LUMO increases

Table 2. Structural data for optimized $[Pt(dien)(Cl)]^+$ in different protocol (Onsager reaction field model). The data are compared with the experimental X-ray crystallographic data.

Bond lengths (Å)	HF	B3LYP	mPW1PW91	Experimental data[b]
Pt-N(T)[a]	2.068	2.076	2.054	2.002(8)
Pt-N_2	2.087	2.078	2.054	2.063(10)
Pt-N_3	2.097	2.088	2.064	2.063(9)
Pt-Cl	2.375	2.330	2.332	2.312(3)
N(T)-C_3	1.498	1.491	1.502	1.48(1)
C_3-C_4	1.530	1.539	1.528	1.53
N(T)-C_5	1.487	1.510	1.491	1.46(2)
N_2-C_3	1.490	1.508	1.4952	1.50(1)
C_5-C_6	1.528	1.536	1.525	1.53
N_3-C_5	1.496	1.508	1.500	1.49(2)
Bond angles(degrees)				
N(T)-Pt-N_2	83.09	84.132	83.89	83.5(4)
N_2-Pt-N_3	83.70	84.78	84.68	84.5(4)
N_2-Pt-Cl	96.79	95.48	95.77	95.6(3)
N_3-Pt-N_2	164.27	165.97	165.90	165.7(4)
N(T)-Pt-Cl	177.90	177.30	177.85	175.6(3)
Dihedral angle(degrees)				
N(T)-C_3-C_4-N_2	40.76	39.96	40.68	-54 ±1
N(T)-C_5-C_6-N_3	51.94	52.20	52.32	-53 ±1

a N(T) is the trans nitrogen with respect to the leaving chloride (Cl^-) ion
b From reference Briton (1992) (for single [Pt(dien)(Cl)]Cl crystal

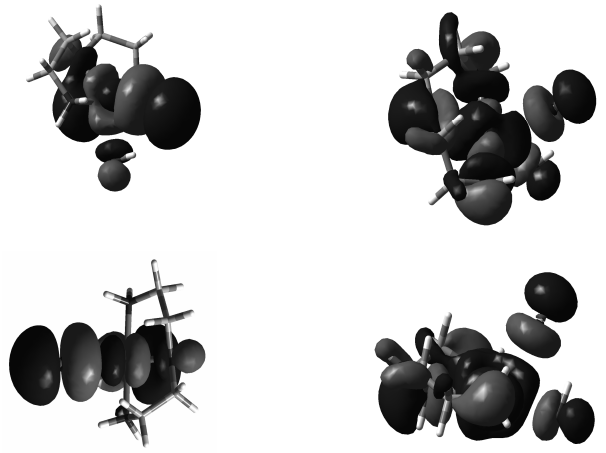

HOMO LUMO

Figure 2a. Isodensity surface of HOMO and LUMO for the TS calculated at the B3LYP level for the nucleophilic path, (Two different views).

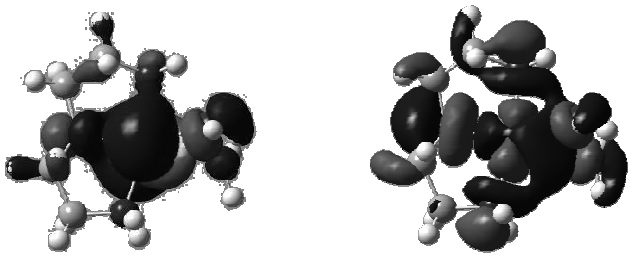

HOMO LUMO

Figure 2b. Isodensity surface of HOMO and LUMO for the TS calculated at the B3LYP level for the solvolytic path.

steadily leading to a decrease in gap between HOMO and LUMO.

Solvolytic path

The Figure 3 shows the existence of all optimized structures of the transition state along with the corresponding reaction intermediate and product intermediate on the potential energy surface for the species involved in the for the solvolytic path. This solvolysis reaction was characterized by replacement of H_2O by H_2O and proceed via a collision between the reactant $[Pt(dien)(H_2O)]^{2+}$ with the solvent H_2O in Onsager self-consistent reaction field model. The TS structure has an imaginary frequency of -160.3 cm^{-1}, computed at B3LYP level of theory. The Pt - O (2.536 Å) bond is breaking and Pt - O (2.499 Å) bond is forming In such substitution process, a five coordinated distorted trigonal bi-pyramid like transition structure, with entering ligand (H_2O), leaving ligand (H_2O) and the metal complex being weakly bound

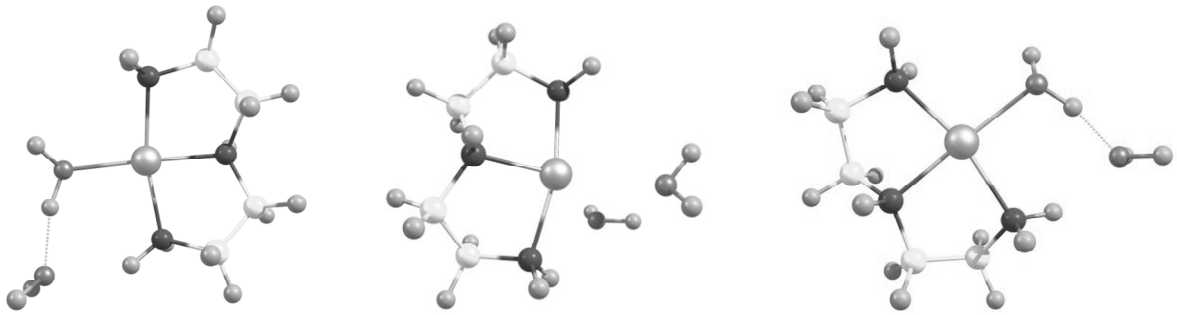

Figure 3. B3LYP optimized structures for species involved in the solvolytic path for the chloride anation reaction of $[Pt(dien)(H_2O)]^{2+}$.

was found. This was found to be true from the structural analysis (Table 2 of supporting information). The small angle between entering H_2O and leaving Cl^- minimizes the repulsion between the d orbital electrons of Pt and the electron pairs of entering and leaving group.

Solvent effect on the structural properties

This section compares the structural data in Onsager self-consistent reaction field model that is, solution phase with the gas phase data for the transition state. All the bond lengths (including Pt…Cl and Pt…OH_2 partial bonds) increase in Onsager model except the equatorial Pt- N bond of the distorted trigonal bi-pyramid like transition state (Table 1). The changes in bond angles are less significant except the equatorial angles. The angle between the entering H_2O and leaving Cl changes significantly from 70.1 to 67.23 degrees. The other two equatorial angle changes their values in all the level of theory concerned. This also favors the conclusion that main geometric change took place in the equatorial plane during the anation process.

Properties of the transition state

Figure 4a and 4b depicts the Fukui functions (f^+), local softness(s) and the energy(E) of the incoming neucleophile (Cl^-) and leaving H_2O along the intrinsic reaction coordinates (IRC) connecting the reactant intermediates, the transition states (TS) and the product intermediates along the minimum energy path. Figure 4(b) depicts the Fukui functions (f^+), local softness(s) and the energy (E) of the solvolytic path (where both incoming and leaving groups are H_2O) along the intrinsic reaction coordinates (IRC) connecting the reactant intermediates, the transition states (TS) and the product intermediates along the minimum energy path. The optimized intermediates were found by full optimization of I and II for both Figure 4a and 4b. The data are superimposed for clear clarification. The nucleophilicity gradually increases for Cl^- (Figure 4a) and H_2O (Figure 4b) and pass through the transition state with an inflection and reach the final level. This indicates that the reactivity depends on the nature and distances of other species present in the transition state (at zero IRC) and is not an absolute property. The reactivity of outgoing H_2O decreases with intrinsic reaction coordinate due to it's involvement in the bond breaking process for the nucleophilic path and ultimately attain a stable closed shell configuration. On the other hand, the reactivity of the chloride ion (Cl^-) increases, passes through the inflection point at IRC zero, due to the formation of Pt - Cl bond. In the transition state, the reactivates of Cl^- and H_2O are same; this implies that the system can proceed to either side on equal ease. The Fukui function of f_k^+ of H_2O and Cl^- coincides at the saddle point and this may be used to locate the transition state for a chemical reaction. This is also true for the solvolytic path.

Energy and activation parameters

The total energy (E) and Gibbs free energy (G) of the intermediate species and the transition state for both the neucleophilic and solvolytic paths are presented in Table 3 and 4. The enthalpy of activation ($\Delta H^{\neq}$) for the nucleophilic path and the entropy of activation ($\Delta S^{\neq}$) for the forward reaction on mPW1PW91 protocol with the general basis set are 54.27 kJ/mol and -37.6 J/K/mol. This is indicative of an associative interchange mechanism for the nucleophilic path (Basolo et al., 1967; Langford et al., 1966). The enthalpy of activation ($\Delta H^{\neq}$) for the nucleophilic path and the entropy of activation ($\Delta S^{\neq}$) for the forward reaction on mPW1PW91 protocol with the general basis set are 54.27 kJ/mol and -37.6 J/K/mol (Table 4 of supporting information). This is indicative of

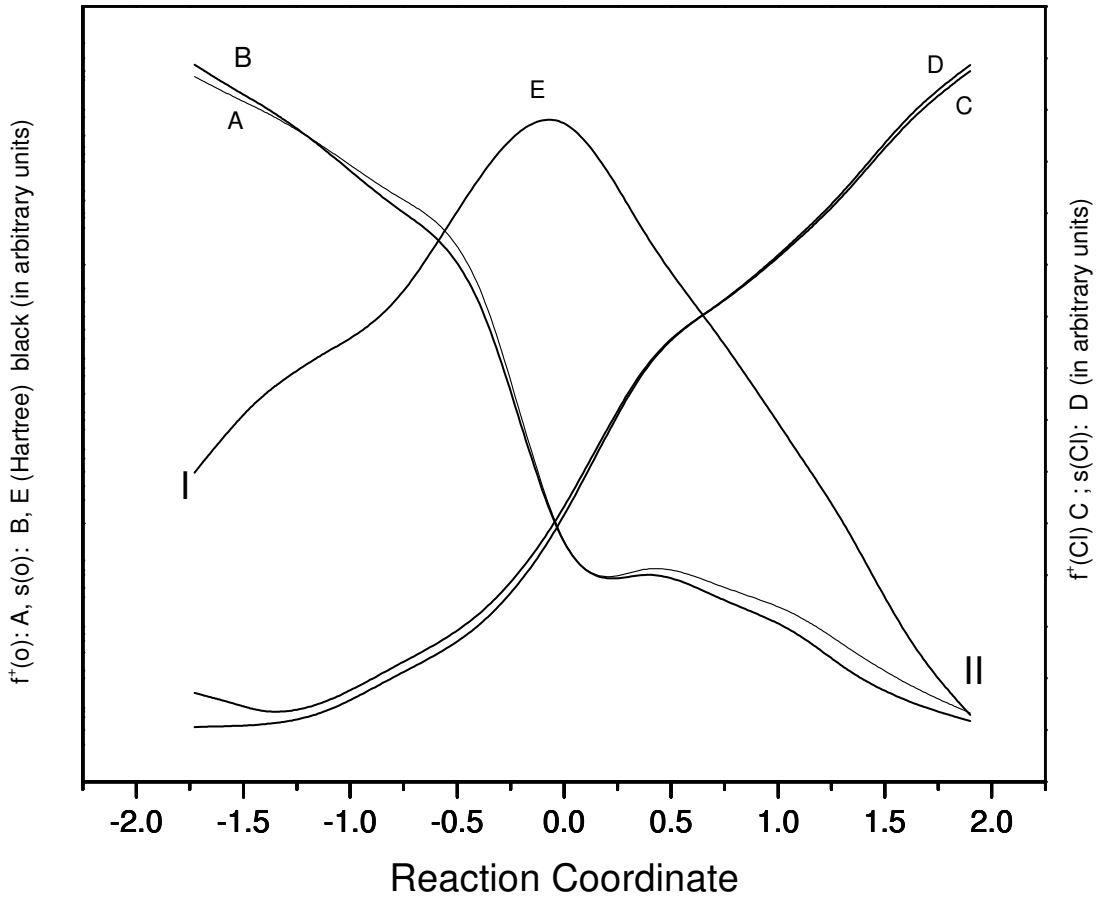

Figure 4a. Profiles of different local reactivity descriptor along the IRC in the nucleophilic path for the chloride anation reaction of $[Pt(dien)(H_2O)]^{2+}$

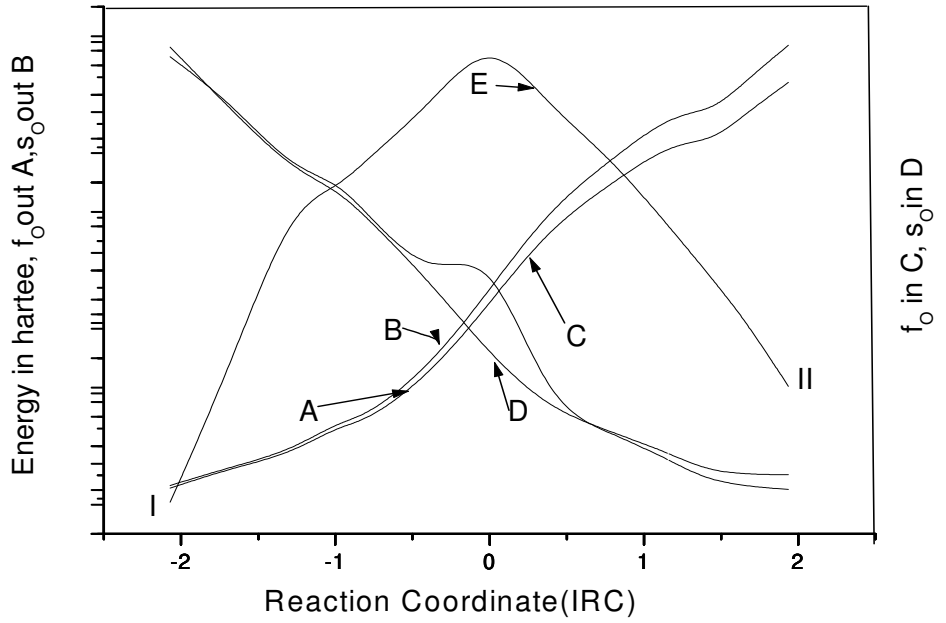

Figure 4b Profiles of different local reactivity descriptor along the IRC in the solvolytic path for the chloride anation reaction of $[Pt(dien)(H_2O)]^{2+}$

Table 3. Total energy (E) and Gibbs Free energy (G), in hartees for the reaction intermediates (**I1** and **I2**) and the transition state of the chloride anation reaction.

		HF	B3LYP	mPW1PW91
I1				
Gas	E	-976.003803	-980.135066	-980.075214
	G	-975.560991	-979.735922	-979.6707803
Onsager	E	-976.045542	-980.166970	-980.101179
	G	-975.605154	-979.764272	-979.696881
TS				
Gas	E	-975.996523	-980.122909	-980.063938
	G	-975.560592	-979.720418	-979.653715
Onsager	E	-976.010203	-980.134484	-980.080130
	G	-975.574876	-979.732079	-979.672822
I2				
Gas	E	-976.038423	-980.165328	-980.1066934
	G	-975.606128	-979.763986	979.700244
Onsager	E	-976.051024	-980.172893	-980.114938
	G	-975.617742	-979.771289	979.707968

Table 4. Total energy (E) and Gibbs free energy (G), in hartees for the reaction intermediates (**I1** and **I2**) and the transition state of the solvolytic reaction.

		HF	B3LYP	mPW1PW91
I1				
Onsager	E	-592.239186	-596.029187	-595.941891
	G	-591.755116	-595.575389	-595.482117
TS				
Onsager	E	-592.208894	-595.993239	-595.905521
	G	-591.726608	-595.543712	-595.449862
I2				
Onsager	E	-592.241316	-596.029098	-595.941859
	G	-591.752263	-595.575872	-595.486048

an associative interchange mechanism for the nucleophilic path.

For solvolytic path, the enthalpy of activation ($\Delta H^{\neq}$) and the entropy of activation ($\Delta S^{\neq}$) values are 82.08 kJ/mol and -8.73 J/K/mol respectively in mPW1PW91 protocol. In the B3LYP protocol, the values are 79.2685 kJ/mol and -12.82 J/K/mol respectively (Table 5 of supporting information). The small negative value for the solvolytic path is a characteristic of the self-exchange associative reaction where both the bond breaking and bond making at the transition state have been playing the important role (Wilkins, 1991).

The rate constants in gas phase for all the protocols are very high this is due to the electrostatic interaction of a bi-positive $[Pt(dien)(H_2O)_2]^{2+}$ ion with the uni-negative Cl^- ion in absence of any retarding force. All the bond lengths increase in Onsager model except the equatorial Pt–O bond of the distorted trigonal-bipyramid-like transition state (**TS** in Figure 1). The changes in bond angle are less significant except the equatorial angle (∠O-Pt-Cl 66.79° in mPW1PW91 protocol). The angle between the entering chloride ion (Cl^-) and the leaving H_2O is almost constant but the other two equatorial angles change their values in all the levels of theory concerned. This also favors the conclusion that main geometric change took place in the equatorial plane during the exchange process.

Conclusion

The extraordinary piece of experimental work of Grey et al. (1962) was experimentally solved after 27 years of the original work and in this paper; we revisited the same chloride anation reaction by *ab-initio* and two DFT methods. The existence of the associative solvolytic path

Table 5. Ratio of rate constants (k_2: k_1) for the nucleophilic path (k_2) and solvolytic path (k_1) are shown in different level of theory of protocol in SCRF (Onsager) model.

Forward reaction		HF	B3LYP	mPW1PW91	Calculated $_{k2/k1}$	Expt $_{k2/k1}$ *
Onsager	k_2	$7.33x10^{-2}$	9.65×10^{-3}	20.69		$1:10^{-4}=10000$
	k_1	18.24	$4.47\ x10^{-2}$	$9.04\ x10^{-3}$	1488.48 (mPW1PW91)	
					0.2158 (B3LYP)	
					0.004 (B3LYP)	
Reverse reaction						
Onsager	k_{-2}	1.18×10^{-7}	5.71×10^{-6}	3.92×10^{-4}		
	k_{-1}	10.35	$1.009\ x10^{-2}$	$1.58\ x10^{-4}$	2.48 (mPW1PW91)	
					$5.7x\ 10^{-4}$(B3LYP)	
					$1.1x10^{-8}$(HF)	

a Reference Grey et al(1962)
Rate constants in sec^{-1}

and the ratio of nucleophilic and solvolytic rate constants (Table 5) are found to be comparable with the result of Marti et al. (1998).

ACKNOWLEDGMENTS

The author thanks the UGC, New Delhi for granting a minor Research Project No. F.PSW-108/06-07, (ERO Sl. No.82420). The author also thanks Dr. Parimal Kumar Das, Dr. T. Storr (Stanford) and Krisnendu Kundu (TIFR), for their cooperation. The author thanks CHEMCRAFT for their free internet version.

REFERENCES

Adamo C, Barone V (1998). Exchange Functionals with Improved Long-Range Behavior and Adiabatic Connection Methods without Adjustable Parameters: The mPW and mPW1PW Models, J. Chem. Phys., 108: 664–675.

Atwood JD (1997). Inorganic and organometallic Reaction mechanisms, 2nd edition, , p.49.

Basolo F, Pearson RG (1967). Mechanisms of inorganic reactions A Study of Metal Complexes in Solutions, John Wiely and Sons, Inc. 2nd edition, p.391.

Becke AD (1988). Density-Functional Exchange-Energy Approximation with Correct Asymptotic Behavior, Phys. Rev. A, 38: 3098–3100.

Becke AD (1993). Density-Functional Thermochemistry. III. The Role of Exact Exchange, J. Chem. Phys. 98: 5648–5652.

Becke AD A new dynamical correlation functional and implications for exact-exchange mixing, J. Chem. Phys. (1996) 104: 1040-1046.

Briton JF, Lock CJL, Pratt WMC (1982). The structures of chloro(diethylenetriamine)platinum(II) chloride and (diethylenetriamine)nitratoplatinum(II) nitrate and some comments on the existence of Pt^{II}-OH_2 and Pt^{II}-OH bonds in the solid state. Acta. Cryst 38: 2148-2155.

Carloni P, Sprik M, Andreoni W J (2000). Phys. Chem B. Structural and Energetic Study of cisplatin and derivatives: Comparison of the Performance of Density Functional Theory Implementations 104: 823-835.

Chattaraj PK Roy DR (2005). A Possible Union of Chemical Bonding, Reactivity, and Kinetics. J. Phys. Chem. A, 110 : 11401–11403.

Cotton FA, Wilkinson G, Murillo CA, Bochmann M (1999). Advanced Inorganic Chemistry Wiley, New York, p. 55

Ditchfield R, Hehre WJ (1971). Pople JA Self-Consistent Molecular-Orbital Methods. IX. An Extended Gaussian-Type Basis for Molecular-Orbital Studies of Organic Molecules, J. Chem. Phys. 54: 724-728

Foresman JB, Ortiz JV, Cui Q, Baboul AG, Clifford S (1996). Exploring chemistry with electronic structure methods, Gaussian, Inc. Pittsburgh, p. 70.

Frisch MJ, Trucks GW, Schlegel HB, Scuseria GE (2004). GAUSSIAN 03, Revision C.02, Gaussian, Inc., Wallingford CT,

Geerlings P, De Profit F (2003). Langenaeker W Computational Density Functional Theory Chem. Rev.103: 1793-1873

Gonzalez C, Schlegel HB (1989). An improved algorithm for reaction path following. J. Chem. Phys. 90: 2154-2161.

Gonzalez C, Schlegel HB (1990). Reaction path following in mass weighted internal coordinates. J. Phys. Chem., 94: 5523-5527

Gray HB, Olcott JR (1962). Kinetics of the reactions of diethylene tri-amineaquoplatinum(II). Inorg. Chem. 1: 481–485

Hay PJ, Wadt WR (1985). Ab-initio effective core potentials for molecular calculations. Potentials for K to Au including the outermost core orbitals. J. Chem. Phys. 82: 299-310.

Hehre WJ, Ditchfield R, Pople JA (1972). Self-Consistent Molecular-Orbital Methods. XII. Further Extensions of Gaussian-Type Basis Sets for Use in Molecular Orbital Studies of Organic Molecules, J. Chem. Phys. 56: 2257-2261.

Langford C, Gray H (1966). Ligand Substition Processes, (Benjamin: New Year,

Kotowski M, Palmer DA, Kelm H (1980). Kinetics of the anation of aquadiethylenetriamineplatinum(II) ions. Kotowski, M., Palmer, D.A.,. Inorg. Chim. Acta. pp. 113-114.

Lewars E (2003). Computational Chemistry, Kluwer Academic Publishers, p 431.

Marti M, Hoa GHB, KoZelka J (1998). Reversible hydrolysis of $[PtCl(dien)]^+$ and $[PtCl(NH_3)_3]^+$. Determination of the rate constants using UV spectrophotometry. Inorg. Chem. Communications. pp. 439-442

Michelle LS, Richard AJ, O'Hair W, McFadyen D , Lily TR, Holmes J,

Robert WG (2000). Formation and gas phase fragmentation reactions of ligand substitution products of platinum (II) complexes via electrospray ionization tandem mass spectrometry. J. Chem. Soc., Dalton Trans pp. 93–99.

Onsager L (1936). Electric Moments of Molecules in Liquids J. Am. Chem. Soc. 58: 1486 -1493

Parr RG, Yang W (1989). Density functional Theory of atoms and molecules, Oxford University Press; pp 66- 96.

Perdew JP, Wang Y (1992). Accurate and Simple Analytic Representation of the Electron-Gas Correlation Energy, Phys. Rev. B,). 45: 13244–13249

Perdew JP, Bruke K, Wang Y (1996). Generalized gradient approximation for the exchange-correlation hole of a many-electron

system, Phys. Rev. B. 54: 16533 -16539.
Szabo A., Ostlund NS (1996). Modern Quantum Chemistry, 1st Edn, revised, McGraw-Hill
Publishing company, New York, p.127
Vosko SH, Wilk L, Nusair M (1980). Accurate Spin-Dependent Electron Liquid Correlation Energies for Local Spin Density Calculations: A Critical Analysis,Can. J. Phys. 58: 1200–1211.
Wadt WR, Hay PJ (1985). Ab-initio effective core potentials for molecular calculations. Potentials for main groups elements Na to Bi. J. Chem. Phys 82: 284 -298.
Wilkins RG (1991). Kinetics and Mechanism of Reactions of Transition Metal Complexes, VCH, Weinheim p.202
Wong MW, Wiberg KBM, Frisch J(1991). Solvent Effects. 1. The Mediation of Electrostatic Effects by Solvent. J. Am. Chem. Soc. 113: 4776-4782.
Wong MW, Wiberg KB (1992). Frisch M J Solvent Effects. 2. Medium Effect on the Structure, Energy, Charge Density, and Vibrational Frequencies of Sulfamic Acid. J. Am. Chem. Soc., 114: 523 - 529.
Wong MW, Wiberg KB (1991). Frisch MJ Hartree-Fock second derivatives and electric field properties in a solvent reaction field: Theory and application. J. Chem. Phys. 95: 8991-8998.
Wong MW, Wiberg KB, Frisch MJ (1992). Solvent Effects. 3. Tautomeric Equilibria of Formamide and 2-Pyridone in the Gas Phase and Solution. An ab Initio SCRF Study J. Am. Chem. Soc. 114: 1645 – 1652.
Wong E, Giandomenico CM (1999). Current status of platinum-based antitumor drugs. Chem Rev 99: 2451-2466.
Zeigler T (1995). The 1994 Alcan Award lecture Density Functional Theory as a practical tool in studies of organometallicenergatics and kinetics. Beating the the heavy metal blues with DFT. Can. J. Chem. 73: 743-760.